Published in final edited form as:
ACS Chem Biol. 2008 September 19; 3(9): 542–554. doi:10.1021/cb800085g.

Gatekeeping *versus* Promiscuity in the Early Stages of the Andrimid Biosynthetic Assembly Line

Nathan A. Magarvey[†,§,¶], **Pascal D. Fortin**[†,¶], **Paul M. Thomas**[‡], **Neil L. Kelleher**[‡], and **Christopher T. Walsh**[†,*]

[†]Department of Biological Chemistry and Molecular Pharmacology, Harvard Medical School, Boston, Massachusetts 02115

[‡]Department of Chemistry, University of Illinois, Urbana–Champaign, Illinois 61801

Abstract

The antibiotic andrimid, a nanomolar inhibitor of bacterial acetyl coenzyme A carboxylase, is generated on an unusual polyketide/nonribosomal pep-tide enzyme assembly line in that all thiolation (T) domains/small-molecule building stations are on separate proteins. In addition, a transglutaminase homologue is used to condense andrimid building blocks together on the andrimid assembly line. The first two modules of the andrimid assembly line yields an octatrienoyl-β-Phe-thioester tethered to the AdmI T domain, with amide bond formation carried out by a free-standing transglutaminase homologue AdmF. Analysis of the aminomutase AdmH reveals its specific conversion from L-Phe to (*S*)-β-Phe, which in turn is activated by AdmJ and ATP to form (*S*)-β-Phe-aminoacyl-AMP. AdmJ then transfers the (*S*)-β-Phe moiety to one of the free-standing T domains, AdmI, but not AdmA, which instead gets loaded with an octatrienoyl group by other enzymes. AdmF, the amide synthase, will accept a variety of acyl groups in place of the octatrienoyl donor if presented on either AdmA or AdmI. AdmF will also use either stereoisomer of phenylalanine or β-Phe when presented on AdmA and AdmI, but not when placed on noncognate T domains. Further, we show the polyketide synthase proteins responsible for the polyunsaturated acyl cap can be bypassed *in vitro* with *N*-acetylcysteamine as a low-molecular-weight acyl donor to AdmF and also *in vivo* in an *Escherichia coli* strain bearing the andrimid biosynthetic gene cluster with a knockout in *admA*.

Microbes have crafted a seemingly endless array of small molecules with diverse structures and biological activities. Chief among the microbial natural product biosynthesis strategies are those based on thiotemplated synthesis involving modular assembly line enzymes such as polyketide synthases (PKSs) and nonribosomal peptide synthetases (NRPSs) or hybrids thereof (1, 2). Each small-molecule assembly machine directs production of a single end product or a relatively small number of highly related congeners. Such biosynthetic fidelity highlights nature's gatekeeping strategies to ensure creation of the evolutionarily selected natural product(s) when environmental cue(s) trigger pathway activation. Teasing apart a biosynthetic sequence to unveil gatekeeper catalysts provides key details on how nature achieves its chemical fidelity. Moreover, as an added benefit, such insight may reveal promiscuous assembly line catalysts that are not part of a biosynthetic guardian system.

[*]Corresponding author, christopher_walsh@hms.harvard.edu.
[§]Current address: Department of Biochemistry and Biomedical Sciences and Department of Chemistry, McMaster University, Hamilton, Ontario, Canada L8N 3Z5.
[¶]These authors contributed equally to this work.

Such enzyme components could serve as entry points to manipulate and redirect assembly lines to create unnatural "antibiotics" with improved activities (1).

Andrimid (structure in Figure 1) and its congener moiramide (hexadienoyl in place of octatrienoyl acyl chain) are hybrid NRP–PK antibiotics that are of intense current interest as molecules that target membrane biosynthesis (3, 4). They do so because they selectively inhibit bacterial over eukaryotic acetyl coenzyme A (CoA) carboxylases *via* blockade of the step catalyzed by the carboxyltransferase subunit, the transfer of CO_2 from *N*-carboxy biotin to the thioester enolate of acetyl CoA en route to malonyl CoA (5). Without a pool of malonyl CoA, essential for Claisen-type fatty acid chain elongation by fatty acid synthases, affected bacteria are unable to make phospholipids as the proximal cause of impaired cell membrane integrity (5, 6).

There are several noteworthy aspects of andrimid biosynthesis. First is the structure of andrimid (and moir-amide). Inspection suggests that three amino acids, phenylalanine, valine, and glycine, are building blocks, each with a twist. The phenylalanine moiety is actually (*S*)-β-Phe, and the valine and glycine residues have been extended by two carbons derived from malonyl units (7). The N-terminus (of the β-Phe residue) is acylated with the octatrienoyl moiety as an N-cap, and the C-terminus of a presumed linear intermediate has been oxidized and cyclized to a methylsuccinimide, which serves as the pharmacophore for carboxyltransferase inhibition (7, 8).

The second feature of note is the six-module hybrid NRPS–PKS assembly line (Figure 1). Each NRPS and PKS module must have a thiolation (T) domain bearing a post-translationally added phosphopantetheinyl arm, as a covalent way station for the growing intermediates predicted to alternate six times between PKS and NRPS logic. The *adm* biosynthetic gene cluster was cloned by Clardy and colleagues (7) into *E. coli* from the producer *Pantoea agglomerans* and detected by bioassay of andrimid. This led to the sequencing of a contiguous 20-kb gene cluster containing *admA-T* and the bioinformatic prediction of the assembly line layout (Figure 1) (7). The hybrid assembly line has three unusual aspects: (i) the distribution of the six T domains over six separate proteins; (ii) the lack of malonyltransferase domains, suggesting the acyltransferase from the producer organism's fatty acid synthase acts *in trans*; and (iii) the absence of NRPS-type condensation (C) domains for the first and second amide bonds, implying a novel type of elongation catalyst for this class of NRP–PK hybrids.

In a prior report, we noted that AdmF, a free-standing transglutaminase homologue, catalyzes the first amide bond and that the congeneric AdmS may catalyze the second as the chain grows (8). We also briefly reported that AdmH can convert L-Phe to β-Phe and that AdmJ can activate the β-Phe (8). In this study, we have focused on additional characterization of the enzymes at the front-end of the andrimid assembly line. These include investigation of AdmH, the methylidene-imidazolone (MIO)-containing aminomutase, and AdmJ, the β-Phe-selecting adenylation (A) domain, as gatekeepers for determining which aromatic amino acid moiety is presented to AdmF as nucleophilic partner (Figure 1). Both AdmA and AdmI are free-standing T domains, and we have examined to what extent AdmJ also acts as a gatekeeper for recognition of either T domain scaffold. In turn, AdmF uses acyl-*S*-T domain as donor and β-aminoacyl-*S*-T domain as acceptor in the amide bond-forming step, so we report on three aspects of recognition of AdmF: for the upstream acyl donor, for the downstream amine acceptor, and for the T domain scaffolds presenting those acyl groups. In this connection, we show that an octatrienoyl-*S*-*N*-acetylcysteamine (*S*-NAC) will work *in vitro* and in recombinant *E. coli* cells for andrimid production in an *admA* knockout.

RESULTS AND DISCUSSION

Gatekeeping at the Start of the Andrimid Assembly Line

The first of the three amino acids used in andrimid assembly is the nonproteinogenic (*S*)-β-Phe, generated by AdmH and then activated and installed on the assembly line by AdmJ. The other two amino acids are proteinogenic, Val_2 and Gly_3, but each undergoes a two-carbon chain extension by PKS modules AdmO and AdmM, respectively. *N*-Capping of andrimid is achieved by the addition of a polyenoic fatty acid moiety tethered on AdmA, resulting in an *N*-acyl-β-Phe amide linkage. Five proteins of the highly disconnected andrimid biosynthetic assembly line are involved in reaching this chain initiation step (Figure 1): the two phosphopantetheinylated T domain proteins AdmA and AdmI, the phenylalanine aminomutase AdmH, the free-standing adenylation domain AdmJ, and the amide-bond-forming AdmF, a transglutaminase homologue (8). To delineate what factors ensure the fidelity in the initial steps of andrimid assembly, the five proteins AdmA, F, I, J, and H were heterologously expressed (8), purified, and assayed for their gatekeeping roles.

AdmH Processes L-Phe to (S)-β-Phe

Previously, we established that AdmH directs β-Phe formation from L-Phe, but the C_3 stereoselectivity of the reaction was not determined (8). AdmH, like other aminomutases, uses an autogenous MIO cofactor that serves as the electrophile for the net movement of the itinerant amino group from C_2 to C_3 of an amino acid (9–11). To assess the ratio of (*R*)-β-Phe *versus* (*S*)-β-Phe formed by AdmH action, assays using [^{14}C]-labeled L-Phe were employed (see Methods). Tracking the progress of the reactions by radio-TLC revealed the time-dependent increase of radioactive β-Phe and corresponding decrease in [^{14}C]-L-Phe (data not shown). The radiolabeled β-Phe product was then subjected to chiral radio-HPLC with conditions resulting in baseline separation of the β-Phe enantiomers (see Methods). Under these chromatographic conditions, authentic standards of (*R*)-β-Phe and (*S*)-β-Phe were retained on the column for 7.2 and 14.8 min, respectively. The β-Phe generated by AdmH was found to be solely (*S*)-β-Phe, because no radioactive compound had a retention time similar to that of authentic (*R*)-β-Phe (Figure 2, panel a). Presumably, this stereo-selectivity achieved by AdmH reflects the chirality control in the addition of ammonia back to the transient cinnamate intermediate in its active site (12). A small amount of radioactivity travels with cinnamate (Figure 2, panel a), an indication that AdmH may also leak cinnamate during enzymatic turnover. The stereocontrol achieved by AdmH is in accord with other MIO-based aminomutase enzymes such as the tyrosine aminomutase SgcC4 from C-1027 enediyne biosynthesis (9) and CmdF aminomutase from chondramide biosynthesis (10). However, CmdF makes the (*R*)-β-Tyr exclusively from L-Tyr (10), whereas SgcC4 makes (*S*)-β-Tyr (9). Presumably, SgcC4 and AdmH orient tyrosine and phenylalanine comparably with respect to the MIO cofactor in these aminomutase active sites. Microbes do not generate (*S*)-β-Phe as part of their primary metabolism. An enantiopure pool created by AdmH would thus be the first gatekeeping mechanism to provide a single diastereomer of the β-amino acid needed to start andrimid synthesis.

AdmJ Prefers (S)-β-Phe Over (R)-β-Phe

AdmJ is a free-standing A domain that activates the (*S*)-β-Phe generated by AdmH action (8. NRPS A domains carry out two-step reactions: they catalyze attack of the amino acid's carboxylate on the electrophilic α-P of ATP to yield tightly bound aminoacyl-AMP in the first step, and then they transfer the activated aminoacyl moiety to the thiolate terminus of the pantetheinyl arm on a cognate T domain.

To determine whether AdmJ has a chiral preference for (*S*)-β-Phe over (*R*)-β-Phe in the first-half reaction, we used the ATP-PP_i radioactive exchange assay and tested both

enantiomers as substrates to drive the equilibration of radioactivity from added $^{32}PP_i$ into ATP. The results of this assay are shown in Figure 2), panel b. A clear preference for (*S*)-β-Phe AMP-ester activation was observed, with only a 2% activation of (*R*)-β-Phe relative to (*S*)-β-Phe. Further characterization of AdmJ revealed the K_m for (*S*)-β-Phe for this exchange reaction to be 130 ± 34 μM, whereas (*R*)-β-Phe was not saturated at 5 mM. SgcC1 also shows micromolar affinity for tyrosine in the comparable assay (13), whereas the chondramide Cmd-A7 A domain has a K_m value for (*R*)-β-Phe in the millimolar range (10). The NRPS code, composed of 10 amino acid residues in A domains, allows for A domain selectivity with respect to α-amino acids (14), but relatively few β-amino acid selecting A domains have been analyzed. Extraction of the AdmJ code (DMLSAKA-MCK) revealed that it is no more similar to that from SgcC1 (DPAQLMLIAK) than the CmdD-A7 A domain code (DGSTITAVAK) (10). Clearly, more sequences of aromatic β-amino-acid-activating A domains are needed to reveal any predictive code that could be used to discriminate an (*S*)- and (*R*)-activating A domain directly from the primary sequence. Like other aromatic β-amino-acid-activating A domains, such as the chondramide β-Tyr A domain from CmdD and the SgcC1 β-tyrosine, AdmJ does not activate the corresponding α-amino acid to any appreciable degree (3% activation of L-Phe relative to (*S*)-β-Phe). The logic used in the enediyne C-1027 and andrimid pathways for generation and installation of (*S*)-β-aromatic amino acids is highly analogous. It is possible this logic is common in microbial natural product pathways using such building blocks.

AdmJ Transfers (*S*)-β-Phe to Holo-AdmI but Not Holo-AdmA

Both SgcC1 and AdmJ activate and deliver an (*S*)-β-amino acid *via in trans* recognition of their T domain partners, an unusual situation that mandates protein – protein recognition between the A and T domains. In most NRPS assembly lines, A and T domains are fused, with the T domain immediately downstream, so the aminoacyl transfer to the thiolate of the phosphopantetheinyl arm of the downstream T domain is at high local concentrations, further assisting amino acid loading. In this highly dissociated andrimid assembly line, AdmJ has to select one of six T domains *in trans* (Figure 1), two of which (AdmA and AdmI) are free-standing. The holo form (HS-pantetheinyl arm) of AdmA should function as an acyl carrier protein (ACP), to be loaded with the octatrienoyl acyl group, while the holo form of AdmI should be the peptidyl carrier protein and receive the (*S*)-β-Phe moiety from AdmJ (Figure 1).

To evaluate AdmJ as a gatekeeper for AdmA *versus* AdmI andrimid assembly in the AdmJ second-half reaction, the formation of [^{14}C]-(*S*)-β-Phe-S-T domains was monitored by autoradiography of proteins on SDS-PAGE gels as shown in Figure 2, panel c. The required [^{14}C]-(*S*)-β-Phe was first created *in situ* from [^{14}C]-labeled L-Phe using AdmH. The [^{14}C]-(*S*)-β-Phe was then mixed with AdmJ, ATP, and either AdmA or AdmI. The radioactive amino acids covalently bound *via* a thio-ester linkage to the pantetheinyl arm of the AdmA or AdmI domains are stable to SDS gel separation. These side-by-side assays, using a fixed amount of AdmJ with equivalent amounts of AdmA or AdmI, showed that AdmJ installs (*S*)-β-Phe to AdmI but not to AdmA (Figure 2, panel c). It is likely that both AdmA and AdmI have the typical four-helix bundle architecture of carrier protein domains (15–19) but that surface residues will control recognition by partner proteins (20, 21).

This selective transfer of (*S*)-β-Phe to AdmI would leave AdmA as an open way station for templated synthesis of the octa-2,4,6-trienoyl moiety by type II PKS proteins encoded by AdmB, C, D, and E. The AdmA and AdmI proteins represent an attractive pair for structure–function analyses to deconvolute recognition determinants by the ketosynthase (KS) AdmD for holo-AdmA *versus* the A domain AdmJ for holo-AdmI.

In sum, these results reveal that the gatekeepers of the early steps in this dissociated assembly line are stereoselective production of (*S*)-β-Phe, chiral specificity of AdmJ for (*S*)-β-Phe, and precise delivery of (*S*)-β-Phe-AMP ester to the holo form of the carrier protein AdmI through selective protein–protein interactions.

Bypass of the Gatekeeper Functions of Adm BCDEHJ: Evaluation of AdmF Condensation Activity When T Domain Scaffolds Are Shuffled

Given the various gatekeeper functions of AdmH and J and the regiospecific enzymatic loading of an octatrienoyl group to the HS-pantetheinyl arm of AdmA and the (*S*)-β-Phe to the pantetheinyl arm of AdmA, we turned to enzymatic loading of the apo forms of the two T domain proteins by phosphopantetheinyltransferase action to present different acyl and aminoacyl groups on the two T domain scaffolds. This approach uses the promiscuity of the *Bacillus subtilis* Sfp to convert apo forms of T domains to acyl-*S*-pantetheinyl forms by post-translational modification with acyl or aminoacyl CoA substrates in a reaction that transfers (amino)acyl-*S*-pantetheinyl-phosphate onto the reactive serine side chain of the apo T domain proteins (22).

As a first experiment, we exchanged the T domain scaffolds to evaluate whether the amide-forming AdmF would accept either AdmA or AdmI as protein scaffold for presentation of an electrophilic or nucleophilic partner in the generation of the *N*-acyl-β-Phe-*S*-T domain assembly line intermediate. To accomplish this, we synthesized (*S*)-β-Phe-CoA and butyryl-CoA and used Sfp to install (*S*)-β-Phe on AdmA instead of AdmI and the butyryl chain on AdmI instead of AdmA. Previously, we established that a butyryl served as an acyl chain surro-gate when presented on AdmA (8). The shuffled electrophilic donor (butyryl-*S*-AdmI) and nucleophilic acceptor ((*S*)-β-Phe-S-AdmA) were then mixed with AdmF. Remarkably, AdmF tolerated this shuffling as evidenced by accumulation of a mass-shifted AdmA at 13,189.5 Da, an indication of transfer of the butyryl group and consistent within 0.1 Da of the expected mass of butyryl-*S*-AdmA (Figure 3). This was further confirmed by elimination of the acylated phosphopantetheine chain in the mass spectrometer, allowing detection of the *N*-acyl-(*S*)-β-Phe-pantetheine elimination product with <1 mDa mass accuracy (23) at 478.2366 Da (theoretical 478.2371 Da, –1.1 ppm error) (data not shown). Supporting this conclusion was the corresponding loss of a butyryl group on AdmI (Figure 3). These are end-point assays, and kinetic analyses are difficult because both substrates and the product are covalently bound to proteins. With that caution, this result shows that AdmF does not require presentation of the acyl chain electrophilic donor or the nucleophilic chain acceptor on the same protein scaffolds (AdmA and AdmI, respectively) upon which they are naturally built. It is plausible that AdmF recognizes an analogous composite surface on AdmA and AdmI (likely made of a combination of the building block small molecule, pantetheinyl arm, and T domain protein) that is distinct from the one recognized by AdmJ.

To evaluate whether the carrier protein scaffold is important for recognition, we tested whether AdmF operates on T domain scaffolds found within other natural product assembly lines. T domains from PKS assembly lines, otherwise known as ACPs, are recognized by KS domains, whereas T domains from NRPS assembly lines are recognized by amide-forming C domains. A selection of T domains from such contexts were used, some naturally free-standing and others excised from multidomain assembly line enzymes. The following seven ACPs found within PKS assembly lines were used: EpoA (epothilone type I PKS), TaB/E (myxovirescin type II PKS), CurB (curacin type I PKS), AcpK (type II PKS), FruJ (frenolicin type II PKS), and EncC (enterocin type II PKS) (24–29). Each apo T domain was incubated with butyryl-CoA and Sfp to install the butyryl-*S*-pantetheinyl moiety, as prior work had shown that a butyryl chain is a substitute for the octatrienoyl chain as acyl donor in AdmF catalysis (8). Coincubation with (*S*)-β-Phe-AdmI and AdmF, followed by Fourier transform mass spectrometry (FTMS) interrogation, did not in any of the various reactions

show AdmI products bearing *N*-acyl-β-Phe (data not shown). To test whether AdmF could work with other NRPS T domains that are protein substrates for C domains, three examples were selected: the well-characterized EntB T domain (enterobactin assembly line), CmaD (a natural free-standing T domain within the cytotriene assembly line), and BarA (a natural free-standing T domain within the barbamide assembly line)(30–32). For these alternative T domains, (*S*)-β-Phe was loaded onto the apo forms using Sfp and (*S*)-β-Phe-CoA. In these assays with butyryl-*S*-AdmA as donor, no butyryl-β-Phe products were detected on the naturally occurring free-standing T domains, CmaD and BarA, but in these assays AdmF had clearly acylated itself on its active site cysteine with the butryl substrate from AdmA, as holo-AdmA accumulated in these assays (data not shown). Further analysis of the EntB T domain loaded with octanoyl-CoA in the presence of (*S*)-β- Phe-S-AdmI and AdmF revealed a small quantity of *N*-octanoyl-(*S*)-β-Phe-S-AdmI, detected by a 126-Da shift from the (*S*)-β-Phe-*S*-AdmI and confirmed by the presence of the *N*-octanoyl-(*S*)-β-Phe-*S*-pantetheine ejection product in these end-point assays (Supplementary Figure 1). Clearly, AdmF does have a built-in bias/selectivity for T domain partners on which it naturally operates, and it may be that the T domain scaffolds of AdmA and AdmI have some recognition surface elements distinct from the other 10 T domains surveyed.

AdmF Specificity toward Alternative Nucleophiles Presented on AdmI

In nature, it would appear, on the basis of the gatekeeping studies described in this work, that AdmF is rarely presented with alternatives to the (*S*)-β-Phe on AdmI. However, for purposes of reprogramming this distributed antibiotic assembly line, it would be useful to know what the tolerance of AdmF would be for donor and acceptor substrates presented on AdmA and AdmI. A first effort involved the two enantiomers of β-Phe and α-Phe, respectively, as nucleophilic partners. For these experiments, L-Phe, D-Phe, and (*R*)-β-Phe (as well as (*S*)-β-Phe, previously noted) were coupled to CoA using coupling chemistries described in Methods. Each of these aminoacyl-CoAs were then used as substrates with Sfp, in conjunction with apo-AdmI as a cosubstrate. In all four cases, AdmI was enzymatically loaded with the corresponding phenylalanine isomer, and the butyryl-*S*-AdmA was used as electrophilic partner. Interrogation of these reactions in end-point assays was achieved by FTMS. AdmF can use (*R*)-β-Phe-AdmI as evidenced by butyryl-(*R*)-β-Phe-*S*-AdmI product (Figure 4). The apparent turnover rate of AdmF using (*S*)-β-Phe-*S*-AdmI as substrate was 30% higher than that using (*R*)-β-Phe-*S*-AdmI (Supplementary Figure 2), illustrating the kinetic competency of both building blocks as amine nucleophiles to *N*-acyl-α-Phe linkages. When AdmF was challenged with versions of α-aminoacyl-*S*-AdmI derived from Land D-Phe,D-Phe also served as a substrate for AdmF and L-Phe to a lesser extent (Figure 4). Next, we tested the need for the phenyl ring side chain by chemoenzymatically loading β-Ala onto apo-AdmI. When β-Ala was substituted in place of β-Phe, AdmF once again was able to tolerate the change, as the expected *N*-acylated product on AdmI (butyryl-β-Ala-*S*-AdmI) accumulated in a time-dependent fashion (Figure 4).

AdmF Specificity toward Alternate Electrophilic Acyl Thioester Donors on AdmA

To date, the only isolated congener to andrimid is moiramide with the octatrienoyl group replaced with a hexadienoyl chain (4). Given a similar/identical assembly line in the moiramide producers, the chain difference would arise from either pro-grammed or improper chain-length control mediated by the proposed andrimid type II PKS chain-length factor found in AdmD. To test whether AdmF is competent for using hexadienoyl-AdmA as an electrophilic acyl donor, hexadienoyl-CoA was synthesized and loaded onto AdmA using Sfp. Mixing hexadienoyl-AdmA with (*S*)-β-Phe-*S*-AdmI and AdmF did lead to hexadienoyl-β-Phe-AdmI product, proving that moiramide synthesis can be initiated by the andrimid assembly line (Figure 5). Next, we used the acyl CoA/Sfp loading methodology on apo-AdmA to present AdmF with acyl chains not likely generated by the *adm* cluster

encoded polyunsaturated fatty acid synthase, including chains lacking unsaturation (*i.e.*, octanoyl, hexanoyl), shorter chains (C_2 and C_4), longer ones (C_{10}, C_{16}), and ones bearing phenyl substituents (phenylacetyl). The results of acyl chain variant assays are shown in Figure 5. Once again, in these endpoint assays, AdmF revealed its ability to process all nine acyl variants as acyl chain donors to (*S*)-β-Phe-*S*-AdmI.

It would appear that AdmF shows sufficient catalytic promiscuity that variant N-acyl-amino groups could be installed at the front end of the andrimid assembly line to produce analogs biosynthetically if they could be presented on AdmA and AdmI. Structure–function studies by medicinal chemists at Bayer AG have indicated that replacement of the octatrienoyl *N*-cap with aryl side chains improves potency and antibiotic range for such andrimid derivatives (6).

Substitution of Acyl-S-NAC Donors for AdmF Catalysis *in Vitro* and *in Vivo*

Redirecting biosynthetic processes is increasingly viewed as an alternative to synthetic preparation of analogs of complex natural product scaffolds that have pharmacologically interesting activities. For polyketide modifications, a common strategy of preparative utility is to redirect PKSs that have been selectively disrupted in one key catalytic step. The engineered pathways are then fed acyl-*S*-NACs as surrogate acyl donors to bypass the blocked step *via* chemical complementation (33–37). Artificially directing biosynthesis has yielded analogs that are not easily prepared through chemical synthesis (34, 35, 38–40). Central to such successes is the ability of KS domains to use *S*-NAC-tethered molecules as substrates and deliver modified building blocks to a given natural product assembly line for further processing.

To reveal whether the transglutaminase homologue AdmF, like KS domains, can act on *S*-NAC-derivatives, we tested whether octatrienoyl-*S*-NAC can be used as a surrogate acyl donor in place of its natural substrate, octatrienoyl-*S*-AdmA. Octatrienoyl-*S*-NAC was prepared, purified, and incubated in the presence of AdmF (Methods). AdmF catalyzes a two-step transfer of the octatrienoyl group from AdmA, first to the thiolate of an active site cysteine residue, Cys90 (8), and then to the amine acceptor on AdmI. To assess the ability of AdmF to use this acyl-*S*-NAC surrogate, in the firsthalf reaction a “top down” MS approach was employed to directly monitor acylation of AdmF with octatrienoyl-*S*-NAC. Incubation with the octatrienoyl-*S*-NAC revealed a shift in a change in AdmF mass from 35,154.5 Da (theoretical apo-AdmF, 35,154.7 Da) to 35273.7 Da (theoretical octatrienoyl-S-AdmF, 35274.8 Da), an increase consistent with its covalent modification with the octatrienoyl chain (Figure 6, panel a). To assess the second-half-reaction, the octatrienoyl-*S*-NAC, AdmF, and (*S*)-β-Phe-AdmI were mixed, and as expected, octatrienoyl-β-Phe-*S*-AdmI product was observed (data not shown). At least in an *in vitro* setting, AdmF, like the PKS KS domains, is competent with an acyl *S*-NAC substrate.

Next, we wished to show whether an acyl-*S*-NAC could be used by AdmF *in vivo*. To test this, we insertionally inactivated *admA* with a chloramphenicol resistance cassette, within the andrimid-gene-cluster-containing cosmid (5194C1). The resulting cosmid was then introduced back into an *E. coli* strain and assayed for its ability to produce andrimid. As expected, the resulting mutant (5194C1dA2) was unable to produce andrimid: a blockage ensured by removal of the AdmA protein scaffold for octatrienoyl-creating AdmC, D, and E type II PKS (Figure 6, panel b). This mutant therefore served as a necessary background. Supplementation of the octatrienoyl-*S*-NAC to 5194C1dA2 culture with octatrienoyl-*S*-NAC yielded culture broths that contained antibiotic activity (Methods). The analysis of the extracts by HPLC, MS (data not shown), and NMR (data not shown) revealed that andrimid was indeed being produced by the mutant supplemented with the *S*-NAC-surrogate (Figure 6, panel b). Of note, the octatrienoyl-*S*-NAC itself did not possess antibiotic activity. This

rescue of andrimid production from the Δ*admA* strain (5194C1dA2) proves that octatrienoyl-*S*-NAC can enter the *E. coli* cell and react with AdmF to enable the andrimid assembly line to proceed. This result suggests that other acyl-*S*-NAC surrogates, including aryl chains that give lower minimum inhibitory concentrations should be used by AdmF *in vivo* to make andrimid analogs with increased antibiotic potency and efficacy.

Conclusion

In summary, we have now dissected gatekeeping functions built into early stages of andrimid assembly. The first gatekeeper is AdmH because it creates an enantiopure pool of (*S*)-β-Phe. The second involves selective recognition of β-Phe over α-Phe by AdmJ and its chiral preference for (*S*) over (*R*)-β-Phe in the aminoacyl-AMP formation step. AdmJ imparts another layer of gatekeeping by discrimination of HS-pantetheinyl forms of AdmA and AdmI, ensuring delivery of (*S*)-β;-Phe to AdmI. We presume, but have not examined, that the AdmC-E proteins, predicted to act in concert as a type II PKS, likewise exhibit specificity for holo-AdmA over holo-AdmI and build an octatrienoyl chain on the former T domain scaffold.

Intermixed within this gated biosynthetic manifold is AdmF, which within its native constrained context would normally be presented with octatrienoyl-AdmA and (*S*)-β-Phe-AdmI. One exception could be a hexadienoyl chain on AdmA, which would result in moiramide production. Although AdmF is not discriminating about which T domain scaffold, AdmA or AdmI, bears the nucleophilic and electrophilic partners for octatrienoyl-β-Phe amide bond formation, it will not use 10 T domains from other microbial PKS or NRPS assembly lines. Use of AdmF as a replacement condensation catalyst in heterologous pathways thus may require import of the AdmA and AdmI scaffolding partners.

The diversity of antibiotic agents in nature is made possible, to a large extent, by the seemingly innumerable combinations of assembly line enzyme permutations allowed by shuffling their corresponding domain components. The atypical and fragmented andrimid assembly machinery suggests it is a recent evolutionary construction. Transglutaminases are known to be a relatively promiscuous enzyme group (41–44). The recruitment of a portable and flexible catalyst such as AdmF to a fragmented assembly line might constitute a diversification experiment in progress. While transglutaminases normally use protein glutaminyl side chains as acyl donors and lysine side chains as nucleophiles (41, 42), AdmF has evolved to use small-molecule substrates tethered as thioesters to carrier protein scaffolds.

Much attention has recently been focused on devising strategies to redirect and rationally engineer natural product pathways based on assembly line logic. Hybrid assembly lines, however, often suffer from an inability to process different monomer building blocks brought to the assembly line *via* module and domain swaps (45). Success in these endeavors has, in some cases, been precluded by an inability of the two previously known assembly line C catalysts (*i.e.*, KS and C domains) to accept noncognate monomer units (46, 47). Our initial characterization of AdmF could prove pivotal to future successes of engineering natural product assembly lines where deployment of promiscuous condensation catalysts could link monomer units not naturally found together. Furthermore, a strategy to capitalize on AdmF's relaxed specificity and redirect the andrimid biosynthesis platform may facilitate the creation of novel bacterial fatty acid biosynthesis inhibitors.

METHODS

Chemicals, Biochemicals, and Molecular Biology

Chemicals were purchased from Sigma-Aldrich, unless otherwise stated. CoAwas obtained from (MBI Biomedicals) and BOC-protected amino acids purchased from Chem-Impex or NovaBiochem. DNA-modifying enzymes were supplied by New England Biolabs. Oligonucleotides were purchased from Integrated DNA Technologies. *E. coli* Top10 and BL21 (DE3) competent cells were from Invitrogen. Standard protein expression plasmids were obtained from Novagen. Ni-NTA Superflow resin was from Qiagen. Standard DNA manipulations were performed according to standard protocol (48). Plasmid isolations were performed using the Qiaprep kit from Qiagen. Gel extractions of DNA fragments and cleanup of DNA amplicons were achieved using QIA-quick PCR Purification Kit. DNA sequencing of cloned andrimid biosynthetic genes was performed on double-stranded plasmid DNA by the Molecular Biology Core Facilities of the Dana Farber Cancer Institute (Boston, MA). FPLC purification of recombinant proteins was achieved on a Akta FPLC (GE Healthcare) equipped with a HiLoad 26/60 Superdex 200 prep grade column using 20 mM Tris-Cl, pH 8.0, and 200 mM NaCl. SDS-PAGE gels were from Bio-Rad. Protein samples were concentrated using 5 and 10 KDa molecular weight cut off Amicon Ultra-15 filtration units from Millipore, and final protein concentrations were determined by the Bradford assay (49).

AdmH Activity Assays and Detection of Reaction Products

AdmH aminomutase reactions were performed in 20 mM tricine, pH 8.25, at 30 °C in the presence of 100μM [^{14}C]-L-Phe for 45–90 min and then analyzed by radio-HPLC using a Beckman Coulter System Gold instrument equipped with a β-Ram module 3 radioisotope detector (IN/US Systems) and a Chirobiotic T2 250 mm × 4.6 mm 5 μm pore column (Advanced Separation Technologies, Inc.). For chiral separations and analysis of AdmH reactions, an isocratic method was used consisting of a water/ ethanol (10:90) solvent mixture, temperature at 22 °C, and a flow rate of 0.8 mL min^{-1}.

ATP-PP$_i$ Exchange Assay for AdmJ A Domain Substrate Specificity

Reactions (100 μL) contained 75 mM Tris, pH 7.5, 10 mM $MgCl_2$, 5 mM TCEP, 5 mM ATP, 1 mM sodium [^{32}P]pyrophosphate (0.18 uCi), 100 μg mL^{-1} bovine serum albumin with 0.75 μM enzyme, and (*S*)-β-Phe, (*R*)-β-Phe, and L-Phe amino acid concentrations ranging from 0.05 to 5.0 mM. Reactions were incubated at RT for 60 min and were quenched by the addition of 500 μL of 1.6% (w/v) activated charcoal, 200 mM tetrasodium pyrophosphate, and 3.5% perchloric acid in water. The charcoal was pelleted by centrifugation and washed twice with 500 μL of 200 mM tetrasodium pyrophosphate and 3.5% perchloric acid in water. The radioactivity bound to the charcoal was then measured by liquid scintillation counting.

Aminoacylation Assays with AdmJ and Andrimid T Domains

Aminoacylation assays to assess *in trans* loading of AdmI and/or AdmA with AdmJ was investigated by incubating phosphopantetheinylated-AdmI or phosphopantetheinylated-AdmA with 10 μM AdmJ, 1 mM ATP and 100 μM [^{14}C]-(*S*)-β-Phe at 30 °C for 60 min. Reactions were quenched by the addition of SDS-loading dye and heated to 90° C and loaded onto a denaturing SDS-PAGE gel for visualization. Proteins separated in the SDS-PAGE gel were transferred to PVDF membrane (0.2 μM) and exposed to BAS-IIIs image plate for ~24 h. Images of the plates were recorded on a Typhoon 9400 variable mode imager (GE Healthcare) followed by analysis with ImageQuant Software.

Synthesis and Purification of Amino Acid and Acyl CoAs and Octatrienoyl-5-NAC

Synthesis of amino acid CoA analogs was achieved by PyBOP coupling chemistries. For each reaction the following were used: 2 equiv of CoA, 4 equiv of PyBOP, 1 equiv of BOC-protected amino acid, and 8 equiv of diisopropylethylamine. Reactions were carried out in 1.5 mL of 50:50 THF/H_2O in a 15 mm × 45 mm dram vial with mixing at RTfor 1 h. The reactions were then subjected to preparative HPLC performed on a Beckman Coulter System Gold instrument equipped with a Phenomenex Luna C18 column (10 μm, 21.20 mm × 250 mm). The conditions for preparative HPLC included a multistep gradient: 0–40% acetonitrile (0–30 min), 40–70% acetonitrile (30–35 min), and 70–100% acetonitile (35–40 min). In these conditions, BOC-protected β-alanine-CoA eluted at 25 min and BOC-protected (*S*)- and (*R*)-β-phenylalanine CoA and L- and D-phenylalanine CoA eluted between 34 and 35 min. Collections of BOC-protected amino acid CoA were then lyopholized, and the dried material was taken up in 1 mL of neat TFA and mixed with stirring for 10 min. Hexadienoyl-CoA was synthesized using a carbonyldiimidazole (CDI) coupling procedure described previously (50), and when available other acyl-CoAs were obtained from Sigma-Aldrich. Synthesis of octatrienoyl-SNAC was achieved using the same parameters as those previously described for the synthesis of hexadienoyl-CoA (8). LCMS identification of products was carried out on a Shimadzu LCMS-QP8000 equipped with two LC-10ADVP liquid chromatography pump modules, a SPD-10AVVP UV–vis detector, a SIL-10ADVP autosampler module, and a Vydac C18 Mass Spec column (5 μM, 2.1 mm × 250 mm).

Loading Amino Acid and Acyl CoAs onto T Domains

Acylation of AdmA was performed using the phosphopantetheinyl transferase Sfp and various CoA analogs according to a previously published protocol (22). Sfp was overexpressed and purified using a previously established protocol (22). When radiolabeled substrates were used such as [^{14}C]butyryl-CoA and [^{14}C]acetyl-CoA, [^{14}C]acetyl-CoA conditions followed those described previously (8).

AdmF Reaction Conditions

AdmF activity assays. The reaction catalyzed by AdmF was investigated by incubating the enzyme with loaded (acetyl, butyryl, hexanoyl, octanoyl, decanoyl, lauryl, palmitoyl, phenylacetyl, (*S*)-β-Phe) AdmA and loaded ((*S*)-β-Phe, (*R*)-β-Phe, L-Phe, D-Phe,β-Ala, Val) AdmI in 50 mM Tris-HCl, pH 7.5, at 25 °C. For the HPLC assays, 50 μM acyl-*S*-AdmA and/or 50 μM (*S*)-β-Phe-*S*-AdmI were incubated with and without 1–2.5 μM AdmF. After 60 min of incubation at 25 °C, 50 mL of the reaction mixture was analyzed by FTMS (see below). For kinetic analysis for parameters of AdmF's use of (*S*)-β-Phe *versus* (*R*)-β-Phe, the reaction was carried out using 50 μM [^{14}C]butyryl-S-AdmA, or [^{14}C]acetyl-S-AdmA, or 50 μM β-Phe-S-AdmI ((*S*)-β-Phe-AdmI, or (*R*)-β-Phe-AdmI) and 1 μM AdmF in a total volume of 200 μL. The excess [^{14}C]butyryl-CoA or [^{14}C]acetyl-CoA and p-Phe were removed by four consecutive washes with 400 mL of 20 mM HEPES, pH 7.5, in an Ultrafree filter microcentrifugal device (5 kDa cutoff; Millipore). Reactions were quenched by the addition of SDS-loading dye and heated to 90 °C and loaded onto a denaturing SDS–PAGE gel for visualization. Proteins separated in the SDS–PAGE gel were transferred to PVDF membrane (0.2 μM) and exposed to a BAS-IIIs image plate for ~24 h and subsequently read by a Typhoon 9400 variable mode imager (GE Healthcare) followed by analysis with ImageQuant Software.

admA Knockout and Octatrienoyl-S-NAC Feeding

The *admA* knockout in the adm clusterwas prepared in the cosmid 2194C1 (7) using a one-step inactivation by PCR products strategy (51). The chloramphenicol resistance marker used to perform the *admA* knockout was amplified from plasmid pKD3 (51) using the

following oligonucleotides: **5admA-for-ko** 5'-ATG AATTGT CAG ACA TTA AAG ATG ACA TAT GAA TAT CCT CCT TAG-3', **3admA-rev-ko** 5'-GAT TGA CAG TGT TTT TCC ATC AAT TCA CTG GTG TAG GCT GGA GCT GCT TCG-3'. For *S*-NAC feedings, the *admA* KO strain was grown in 1 L of Luria broth (LB) containing 100 μg mL^{-1} ampicillin in a 4-L Erlenmeyer flask with constant shaking (175 rpm) at 30 °C until an OD_{600} ~0.8. Once at OD_{600} 0.8, the culture was supplemented with octatrienoyl-*S*-NAC (dissolved in DMSO) to a final concentration of 2 mM, and the culture was further incubated with shaking for 16 h. The culture was then extracted with an equal volume of ethyl acetate and the organic phase concentrated on a rotaevaporator yielding an extract for biological testing. Extracts were spotted onto 5 mm cellulose filter disks, which were then placed onto an LB agar plate that had been sprayed with the indicator strain *E. coli* IMP (pKM079) (52). Controls included culture extracts of *E. coli* XL-1 Blue MR transformed with 5194C1 (positive control) or pSupercos1 (negative control).

Top-Down FTMS Interrogation of AdmF

Octatrienoyl-*S*-AdmF was prepared through incubation of 20 μM AdmF with 100 μM octatrienoyl-*S*-NAC in 50 mM Tris, pH 7.0 for 30 min. The reaction mixture was purified with a C_4 ZipTip (Millipore) and eluted in 78% acetonitrile, 21% water, 1% formic acid. This mixture was then infused using a Triversa NanoMate (Advion Bio-Sciences) into an LTQ-FT-Ultra mass spectrometer (Thermo Fisher Scientific) operating at 12 T. The 35+ charge state was isolated in the ion trap and detected at 340,000 nominal resolving power at m/z 400.

LC-FTMS Interrogation of T Domains

AdmF-catalyzed reactions were prepared as above and separated on a 1 mm × 150 mm Jupiter C4 HPLC column (Phenomenex) before infusion into a 12 T LTQ-FT Ultra mass spectrometer. Alternating full and source induced dissociation (for pantetheinyl ejection) scans were obtained over a 20-min linear gradient from 40% acetonitrile in water with 0.1 %formic acid to 90% acetonitrile in water with 0.1% formic acid. Identity of the (amino)acyl-*S*-thiolation domains was determined by both the absolute mass shift from the holo enzyme and co-occurrence of the (amino)acyl-*S*-pantetheinyl ejection product (23).

Supplementary Material

Refer to Web version on PubMed Central for supplementary material.

Acknowledgments

We thank J. Clardy for providing cosmid 5194C1 and J. Lai, C. Calderone, D. Galonic, and F. Valliancourt for various assembly line T domains. This work was supported in part by National Institutes of Health Grants GM20011 (C.T.W.) and GM067725 (N.L.K.) and an Institutional Training Grant at the Chemistry/Biology Interface to the University of Illinois GM070421 (P.M.T.).

REFERENCES

1. Walsh CT. Polyketide and nonribosomal peptide antibiotics: modularity and versatility. Science (New York, NY). 2004; 303:1805–1810.
2. Fischbach MA, Walsh CT. Assembly-line enzymology for polyketide and nonribosomal peptide antibiotics: logic, machinery, and mechanisms. Chem. Rev. 2006; 106:3468–3496. [PubMed: 16895337]
3. Fredenhagen A, Tamura SY, Kenny PTM, Komura H, Naya Y, Nakanishi K, Nishiyama K, Sugiura M, Kita H. Andrimid, a new peptide antibiotic produced by an intracellular bacterial symbiont isolated from a brown planthopper. J. Am. Chem. Soc. 1987; 109:4409–4411.

4. Needham J, Kelly MT, Ishige M, Andersen RJ. Andrimid and moiramides A–C, metabolites produced in culture by a marine isolate of the bacterium *Pseudomonas fluorescens:* structure elucidation and biosynthesis. J. Org. Chem. 1994; 59:2058–2063.
5. Freiberg C, Brunner NA, Schiffer G, Lampe T, Pohlmann J, Brands M, Raabe M, Habich D, Ziegelbauer K. Identification and characterization of the first class of potent bacterial acetyl-CoA carboxylase inhibitors with antibacterial activity. J. Biol. Chem. 2004; 279:26066–26073. [PubMed: 15066985]
6. Pohlmann J, Lampe T, Shimada M, Nell PG, Pernerstorfer J, Svenstrup N, Brunner NA, Schiffer G, Freiberg C. Pyrrolidinedione derivatives as antibacterial agents with a novel mode of action. Bioorg. Med. Chem. Lett. 2005; 15:1189–1192. [PubMed: 15686939]
7. Jin M, Fischbach MA, Clardy J. A biosynthetic gene cluster for the acetyl-CoA carboxylase inhibitor andrimid. J. Am. Chem. Soc. 2006; 128:10660–10661. [PubMed: 16910643]
8. Fortin PD, Walsh CT, Magarvey NA. A transglutaminase homologue as a condensation catalyst in antibiotic assembly lines. Nature. 2007; 448:824–827. [PubMed: 17653193]
9. Christenson SD, Liu W, Toney MD, Shen B. A novel 4-methylideneimidazole-5-one-containing tyrosine aminomutase in enediyne antitumor antibiotic C-1027 biosynthesis. J. Am. Chem. Soc. 2003; 125:6062–6063. [PubMed: 12785829]
10. Rachid S, Krug D, Weissman KJ, Muller R. Biosynthesis of (*R*)-beta-tyrosine and its incorporation into the highly cytotoxic chondramides produced by *Chondromyces crocatus* . J. Biol. Chem. 2007; 282:21810–21817. [PubMed: 17545150]
11. Walker KD, Klettke K, Akiyama T, Croteau R. Cloning, heterologous expression, and characterization of a phenylalanine aminomutase involved in Taxol biosynthesis. J. Biol. Chem. 2004; 279:53947–53954. [PubMed: 15494399]
12. Christianson CV, Montavon TJ, Festin GM, Cooke HA, Shen B, Bruner SD. The mechanism of MIO-based aminomutases in β-amino acid biosynthesis. J. Am. Chem. Soc. 2007; 129:15744–15745. [PubMed: 18052279]
13. Van Lanen SG, Lin S, Dorrestein PC, Kelleher NL, Shen B. Substrate specificity of the adenylation enzyme SgcC1 involved in the biosynthesis of the enediyne antitumor antibiotic C-1027. J. Biol. Chem. 2006; 281:29633–29640. [PubMed: 16887797]
14. Stachelhaus T, Mootz HD, Marahiel MA. The specificity-conferring code of adenylation domains in nonribosomal peptide synthetases. Chem. Biol. 1999; 6:493–505. [PubMed: 10421756]
15. Crump MP, Crosby J, Dempsey CE, Parkinson JA, Murray M, Hopwood DA, Simpson TJ. Solution structure of the actinorhodin polyketide synthase acyl carrier protein from *Streptomyces coelicolor* A3(2). Biochemistry. 1997; 36:6000–6008. [PubMed: 9166770]
16. Koglin A, Mofid MR, Lohr F, Schafer B, Rogov VV, Blum MM, Mittag T, Marahiel MA, Bernhard F, Dotsch V. Conformational switches modulate protein interactions in peptide antibiotic synthetases. Science (New York, NY). 2006; 312:273–276.
17. Li Q, Khosla C, Puglisi JD, Liu CW. Solution structure and backbone dynamics of the holo form of the frenolicin acyl carrier protein. Biochemistry. 2003; 42:4648–4657. [PubMed: 12705828]
18. Weber T, Baumgartner R, Renner C, Marahiel MA, Holak TA. Solution structure of PCP, a prototype for the peptidyl carrier domains of modular peptide synthetases. Structure. 2000; 8:407–418. [PubMed: 10801488]
19. Wong HC, Liu G, Zhang YM, Rock CO, Zheng J. The solution structure of acyl carrier protein from *Mycobacterium tuberculosis*. J. Biol. Chem. 2002; 277:15874–15880. [PubMed: 11825906]
20. Lai JR, Fischbach MA, Liu DR, Walsh CT. Localized protein interaction surfaces on the EntB carrier protein revealed by combinatorial mutagenesis and selection. J. Am. Chem. Soc. 2006; 128:11002–11003. [PubMed: 16925399]
21. Lai JR, Koglin A, Walsh CT. Carrier protein structure and recognition in polyketide and nonribosomal peptide biosynthesis. Biochemistry. 2006; 45:14869–14879. [PubMed: 17154525]
22. Quadri LE, Weinreb PH, Lei M, Nakano MM, Zuber P, Walsh CT. Characterization of Sfp, a *Bacillus subtilis* phosphopantetheinyl transferase for peptidyl carrier protein domains in peptide synthetases. Biochemistry. 1998; 37:1585–1595. [PubMed: 9484229]
23. Dorrestein PC, Bumpus SB, Calderone CT, Garneau-Tsodikova S, Aron ZD, Straight PD, Kolter R, Walsh CT, Kelleher NL. Facile detection of acyl and peptidyl intermediates on thiotemplate

carrier domains *via* phosphopantetheinyl elimination reactions during tandem mass spectrometry. Biochemistry. 2006; 45:12756–12766. [PubMed: 17042494]

24. Chang Z, Sitachitta N, Rossi JV, Roberts MA, Flatt PM, Jia J, Sherman DH, Gerwick WH. Biosynthetic pathway and gene cluster analysis of curacin A an antitubulin natural product from the tropical marine cyanobacterium *Lyngbya majuscula*. J. Nat. Prod. 2004; 67:1356–1367. [PubMed: 15332855]
25. Butcher RA, Schroeder FC, Fischbach MA, Straight PD, Kolter R, Walsh CT, Clardy J. The identification of bacillaene, the product of the PksX megacomplex in *Bacillus subtilis*. Proc. Natl. Acad. Sci. USA. 2007; 104:1506–1509. [PubMed: 17234808]
26. Bibb MJ, Sherman DH, Omura S, Hopwood DA. Cloning, sequencing and deduced functions of a cluster of Streptomyces genes probably encoding biosynthesis of the polyketide antibiotic frenolicin. Gene. 1994; 142:31–39. [PubMed: 8181754]
27. Simunovic V, Zapp J, Rachid S, Krug D, Meiser P, Muller R. Myxovirescin A biosynthesis is directed by hybrid polyketide synthases/nonribosomal peptide synthetase, 3-hydroxy-3-methylglutaryl-CoA synthases, and trans-acting acyltransferases. ChemBioChem. 2006; 7:1206–1220. [PubMed: 16835859]
28. Tang L, Shah S, Chung L, Carney J, Katz L, Khosla C, Julien B. Cloning and heterologous expression of the epothilonegene cluster. Science (New York, NY). 2000; 287:640–642.
29. Piel J, Hertweck C, Shipley PR, Hunt DM, Newman MS, Moore BS. Cloning, sequencing and analysis of the enterocin biosynthesis gene cluster from the marine isolate *'Streptomyces maritimus':* evidence for the derailment of an aromatic polyketide synthase. Chem. Biol. 2000; 7:943–955. [PubMed: 11137817]
30. Chang Z, Flatt P, Gerwick WH, Nguyen VA, Willis CL, Sherman DH. The barbamide biosynthetic gene cluster: a novel marine cyanobacterial system of mixed polyketide synthase (PKS)-non-ribosomal peptide synthetase (NRPS) origin involving an unusual trichloroleucyl starter unit. Gene. 2002; 296:235–247. [PubMed: 12383521]
31. Liu J, Duncan K, Walsh CT. Nucleotide sequence of a cluster of *Escherichia coli* enterobactin biosynthesis genes: identification of *entA* and purification of its product 2,3-dihydro-2,3-dihydroxybenzoate dehydrogenase. J. Bacteriol. 1989; 171:791–798. [PubMed: 2521622]
32. Bender CL, Liyanage H, Palmer D, Ullrich M, Young S, Mitchell R. Characterization of the genes controlling the biosynthesis of the polyketide phytotoxin coronatine including conjugation between coronafacic and coronamic acid. Gene. 1993; 133:31–38. [PubMed: 8224892]
33. Jacobsen JR, Hutchinson CR, Cane DE, Khosla C. Precursor-directed biosynthesis of erythromycin analogs by an engineered polyketide synthase. Science (New York, NY). 1997; 277:367–369.
34. Jacobsen JR, Keatinge-Clay AT, Cane DE, Khosla C. Precursor-directed biosynthesis of 12-ethyl erythromycin. Bioorg. Med. Chem. Lett. 1998; 6:1171–1177.
35. Kennedy J. Mutasynthesis, chemobiosynthesis, and back to semi-synthesis: combining synthetic chemistry and biosynthetic engineering for diversifying natural products. Nat Prod. Rep. 2008; 25:25–34. [PubMed: 18250896]
36. Weist S, Sussmuth RD. Mutational biosynthesis–a tool for the generation of structural diversity in the biosynthesis of antibiotics. Appl. Microbiol. Biotechnol. 2005; 68:141–150. [PubMed: 15702315]
37. Moore BS, Hertweck C. Biosynthesis and attachment of novel bacterial polyketide synthase starter units. Nat Prod. Rep. 2002; 19:70–99. [PubMed: 11902441]
38. Kalaitzis JA, Izumikawa M, Xiang L, Hertweck C, Moore BS. Mutasynthesis of enterocin and wailupemycin analogues. J. Am. Chem. Soc. 2003; 125:9290–9291. [PubMed: 12889947]
39. Cropp TA, Wilson DJ, Reynolds KA. Identification of a cyclohexylcarbonyl CoA biosynthetic gene cluster and application in the production of doramectin. Nat. Biotechnol. 2000; 18:980–983. [PubMed: 10973220]
40. Ziehl M, He J, Dahse HM, Hertweck C. Mutasynthesis of aureonitrile: an aureothin derivative with significantly improved cytostatic effect. Angew. Chem., Int. Ed. 2005; 44:1202–1205.
41. Lorand L, Graham RM. Transglutaminases: crosslinking enzymes with pleiotropic functions. Nat. Rev. Mol. Cell. Biol. 2003; 4:140–156. [PubMed: 12563291]

42. Lorand L, Parameswaran KN, Stenberg P, Tong YS, Velasco PT, Jonsson NA, Mikiver L, Moses P. Specificity of guinea pig liver transglutaminase for amine substrates. Biochemistry. 1979; 18:1756–1765. [PubMed: 35225]
43. Taki M, Shiota M, Taira K. Transglutaminase-mediated N- and C-terminal fluorescein labeling of a protein can support the native activity of the modified protein. Protein Eng., Des. Sel. 2004; 17:119–126. [PubMed: 15047907]
44. Ohtsuka T, Sawa A, Kawabata R, Nio N, Motoki M. Substrate specificities of microbial transglutaminase for primary amines. J. Agric. Food Chem. 2000; 48:6230–6233. [PubMed: 11141280]
45. Fischbach MA, Lai JR, Roche ED, Walsh CT, Liu DR. Directed evolution can rapidly improve the activity of chimeric assembly-line enzymes. Proc. Natl. Acad. Sci. U.S.A. 2007; 104:11951–11956. [PubMed: 17620609]
46. Belshaw PJ, Walsh CT, Stachelhaus T. Aminoacyl-CoAs as probes of condensation domain selectivity in nonribosomal peptide synthesis. Science (New York, NY). 1999; 284:486–489.
47. Watanabe K, Wang CC, Boddy CN, Cane DE, Khosla C. Understanding substrate specificity of polyketide synthase modules by generating hybrid multimodular synthases. J. Biol. Chem. 2003; 278:42020–42026. [PubMed: 12923197]
48. Sambrook, J.; Russell, D. Molecular Cloning: A Laboratory Manual. 3rd ed.. New York: Cold Spring Harbor Laboratory Press; 2000.
49. Bradford MM. A rapid and sensitive method for the quantitation of microgram quantities of protein utilizing the principle of protein-dye binding. Anal. Biochem. 1976; 72:248–254. [PubMed: 942051]
50. Tonge PJ, Anderson VE, Fausto R, Kim M, Pusztai-Carey M, Carey PR. Localized electron polarization in a substrate analog binding to the active site of enoyl-CoA hydratase: Raman spectroscopic and conformational analyses of rotamers of hexadienoyl thiolesters. Biospectroscopy. 1995; 1:387–394.
51. Datsenko KA, Wanner BL. One-step inactivation of chromosomal genes in *Escherichia coli* K-12 using PCR products. Proc. Natl. Acad. Sci. U.S.A. 2000; 97:6640–6645. [PubMed: 10829079]
52. Sampson BA, Misra R, Benson SA. Identification and characterization of a new gene of *Escherichia coli* K-12 involved in outer membrane permeability. Genetics. 1989; 122:491–501. [PubMed: 2547691]

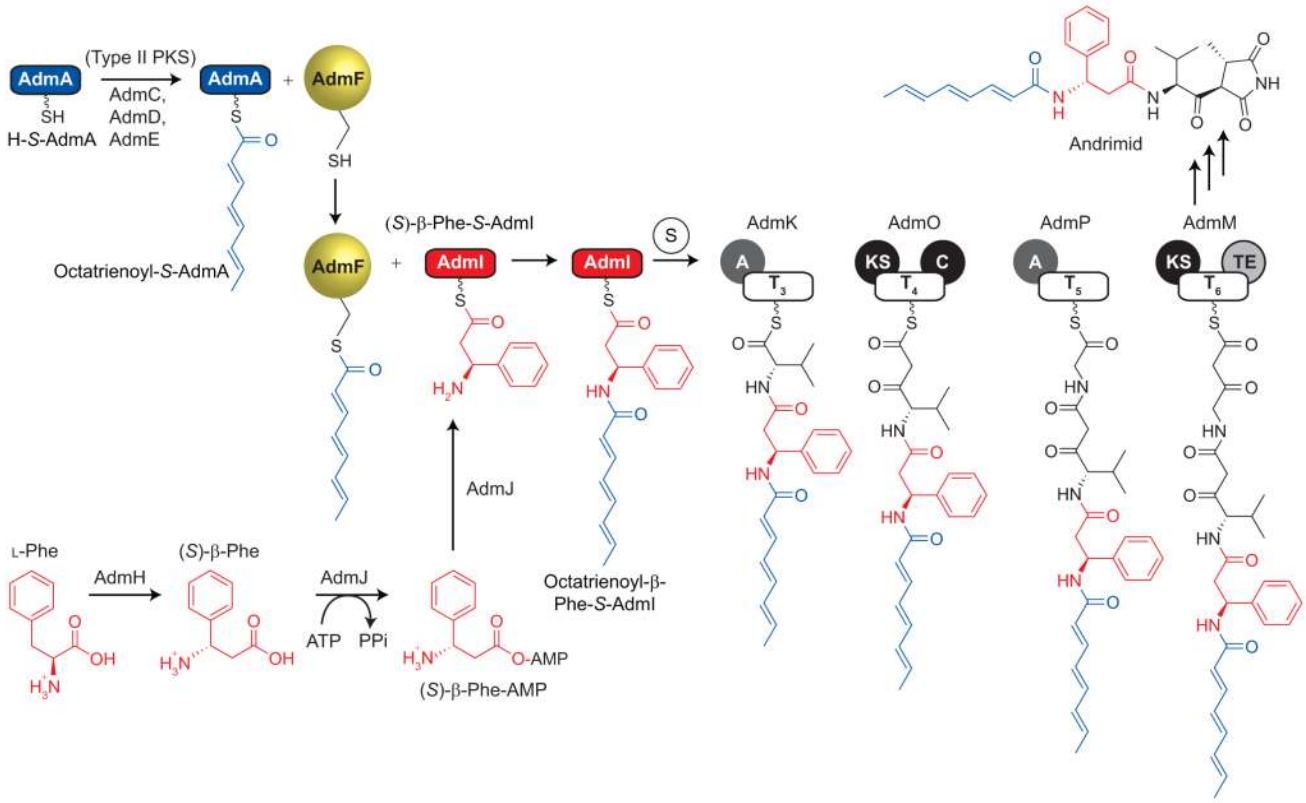

Figure 1.

Highly dissociated biosynthetic pathway of andrimid. The early biosynthetic steps are emphasized. The polyunsaturated acyl chain is installed onto the phosphopantetheinyl (Ppant) arm of holo-AdmA (HS-AdmA) through the actions of a type II PKS. The resulting octatrienoyl-*S*-AdmA (blue) serves as substrate for the self-acylating transglutaminase homologue AdmF (yellow). (*S*)-β-Phe is synthesized from L-Phe by the MIO-containing aminomutase AdmH and is activated to the corresponding AMP-ester by the A domain AdmJ. AdmJ then installs (*S*)-β-Phe onto the Ppant arm of holo-AdmI (HS-AdmI), leading to the formation of (*S*)-β-Phe-*S*-AdmI (red). AdmF catalyzes the formation of an isopeptide bond between the octatrienoyl chain and the amine group of α-phenylalanine through the acylation of its active site cysteine (Cys90). The hybrid biosynthetic pathway proceeds through six T domains before final tailoring leads to the maturation of the final andrimid antibiotic.

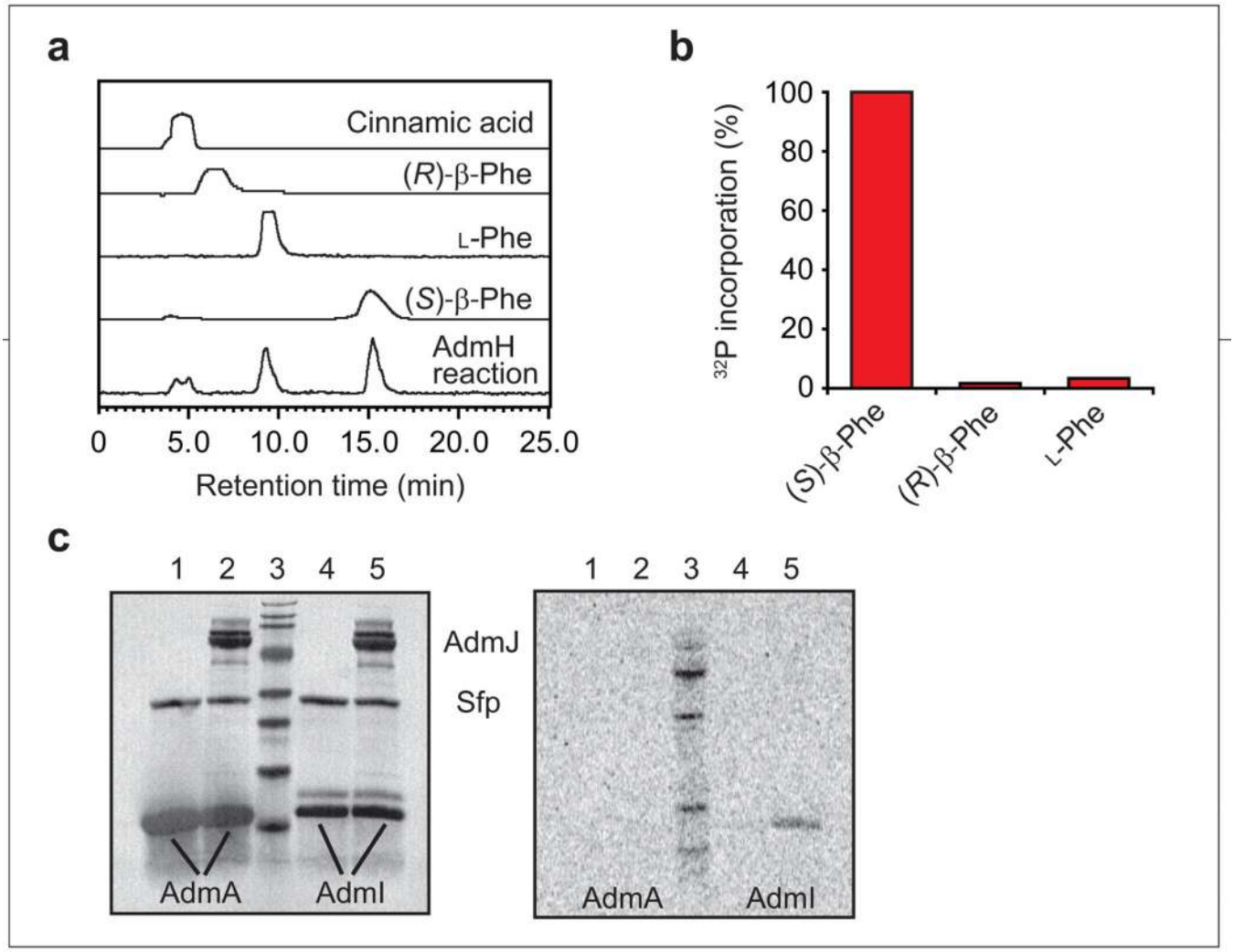

Figure 2.

Early gatekeepers in the biosynthesis and loading of the phenylalanine building block. a) HPLC traces of the AdmH aminomutase reaction. The AdmH reaction was carried out for 90 min at 30 °C using [^{14}C]-labeled L-Phe as substrate. Non-labeled cinnamic acid, (*S*)-β-Phe, and (*R*)-β-Phe and [^{14}C]-labeled L-Phe were used as standards. The AdmH reaction and standards were analyzed by chiral HPLC using an Astec Chirobiotic T2 column and a 9:1 (methanol/water) solvent system. The AdmH reaction produced (*S*)-β-Phe and cinnamic acid. b) Adenylation of phenyla-nine isomers by AdmJ. ATP/pyrophosphate assay carried out using (*S*)-β-Phe, (*R*)-β-Phe, and L-Phe. c) AdmJ-catalyzed loading of (*S*)-β-Phe on AdmI and AdmA. [^{14}C]-labeled (*S*)-β-Phe was incubated with holo-AdmA in the absence and presence of AdmJ (lanes 1 and 2, respectively). [^{14}C]-labeled (*S*)-β-Phe was incubated with holo-AdmI in the absence and presence of AdmJ (lanes 4 and 5, respectively). All reactions were quenched after 60 min of incubation at 30 °C. Left, SDS–PAGE; right, autoradiogram.

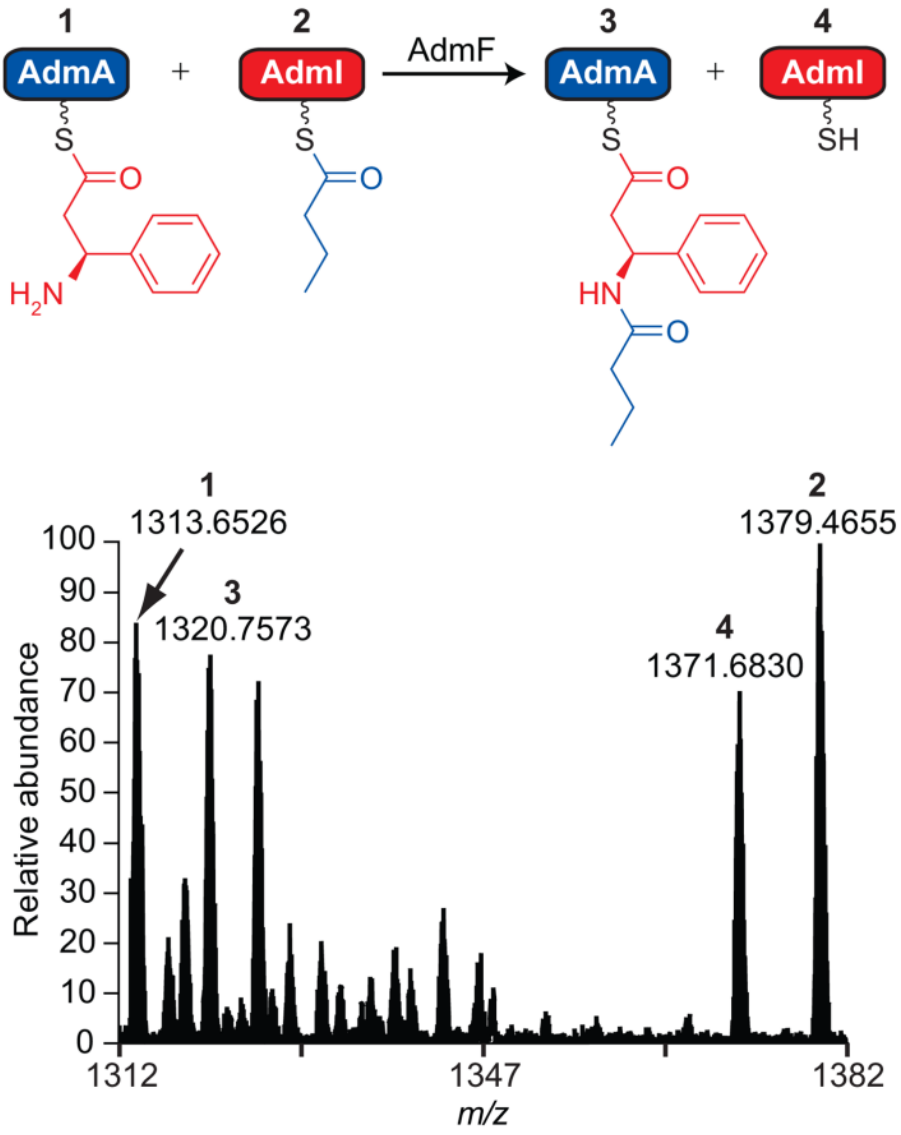

Figure 3.

FT mass spectrum of the reverse AdmF reaction. Shown are the 10+ charge state of AdmA and the 9+ charge state of AdmI. The butyryl chain and (*S*)-β-Phe were loaded onto the reciprocal thiolation domain AdmI (peak 2) and AdmA (peak 1), respectively. The AdmF reaction led to the formation of two products, holo-AdmI (peak 3) and butyryl-(*S*)-β-Phe-S-AdmA (peak 4). Product formation was confirmed by observation of the butyryl-(*S*)-β-Phe-S-pantetheine ejection product within 2 ppm mass accuracy.

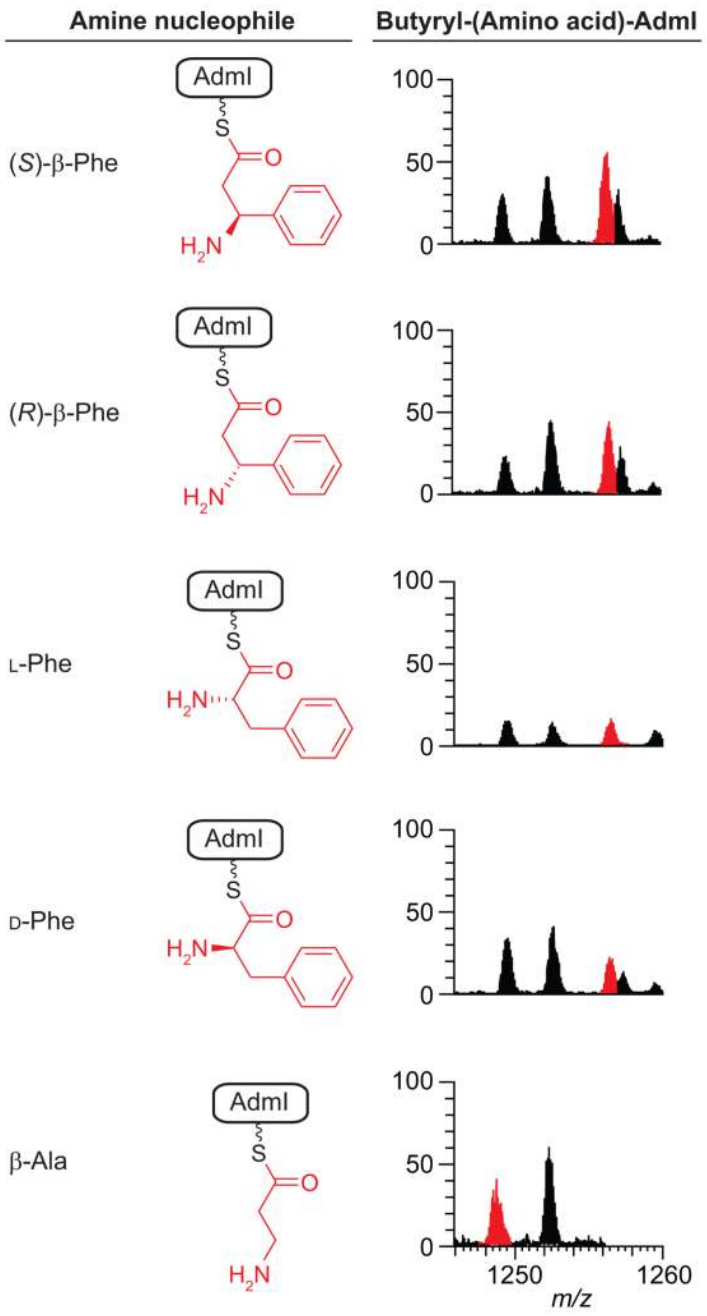

Figure 4.

Recognition of amine nucleophiles by AdmF. FT mass spectrum (10+ charge state) of the AdmF reaction products arising from the isopeptide formation between the acyl chain of butyryl-*S*-AdmA and aminoacyl-*S*-AdmI. AdmI was loaded with the amine donors (*S*)-β-Phe, (*R*)-β-Phe, D-Phe, L-Phe, and (*S*)-β-Ala (top to bottom). All reactions were quenched after 30 min of incubation at 30 °C.

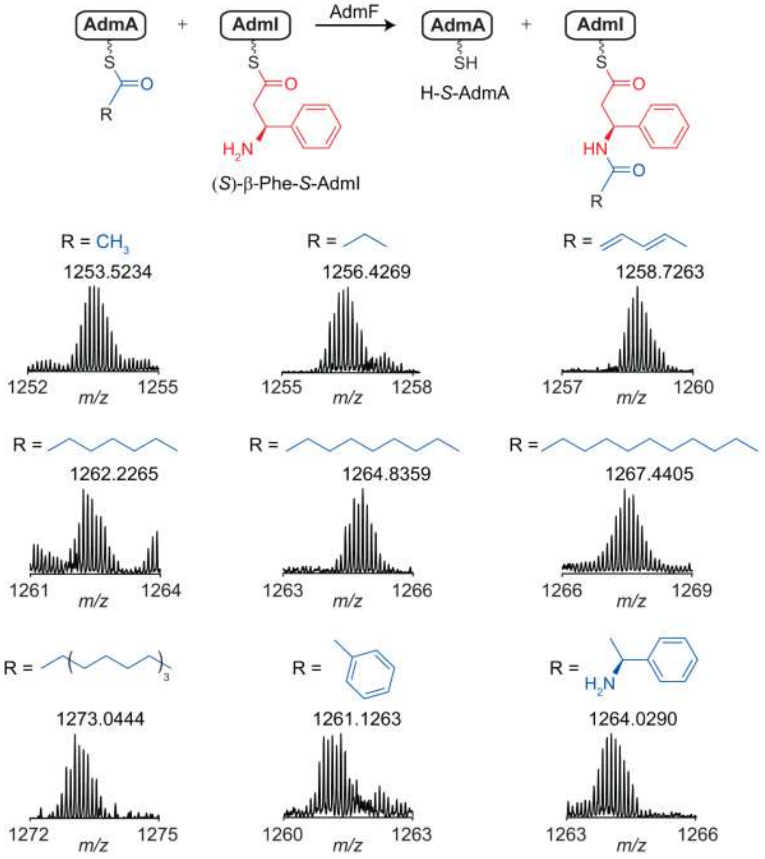

Figure 5.

AdmF accepts a wide array of acyl chain donors. FT mass spectra of the AdmF reaction products obtained using AdmA T domains loaded with the following acyl chain donors with (*S*)-β-Phe-*S*-AdmI.

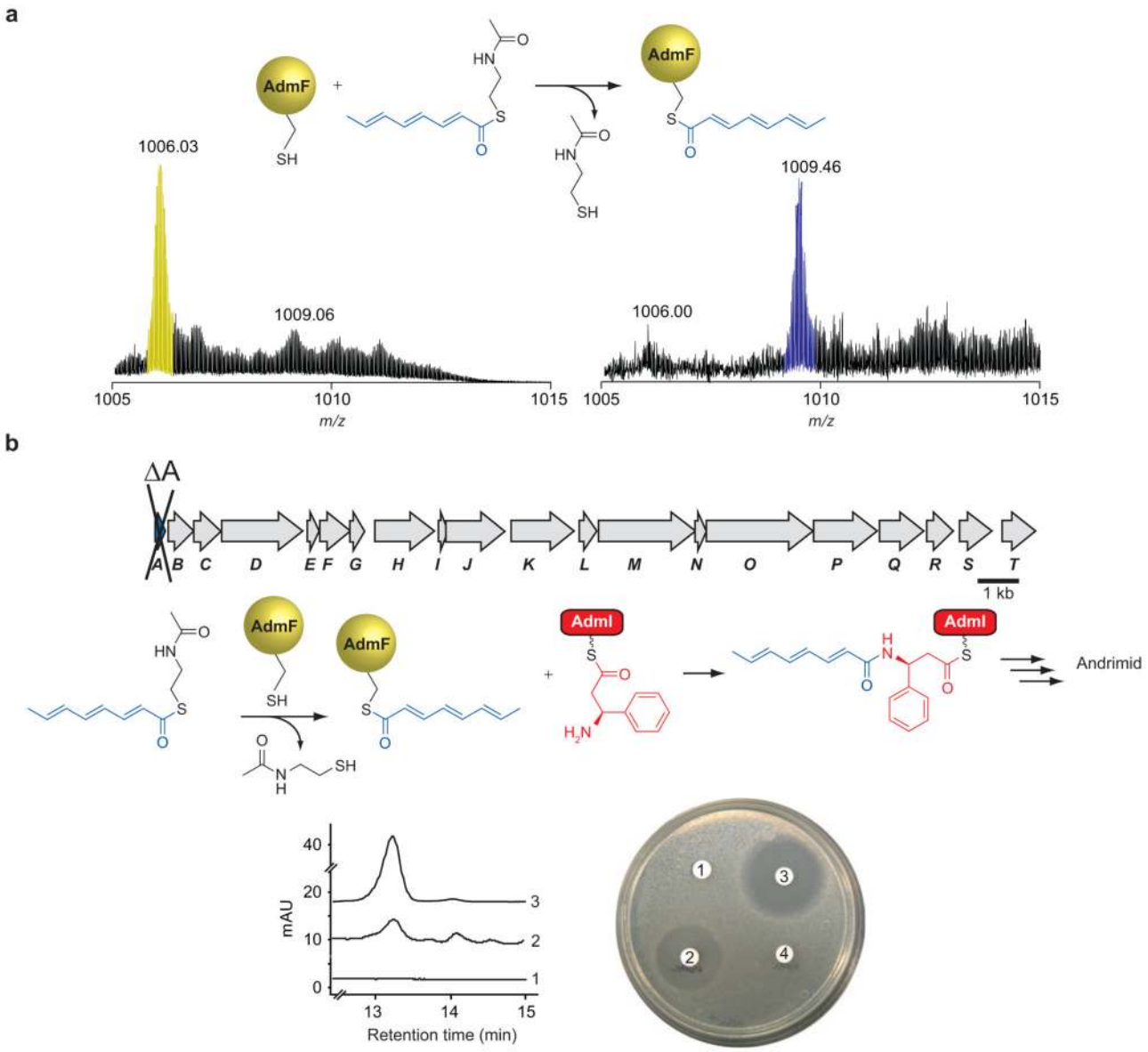

Figure 6.

AdmF accepts octatrienoyl-*S*-NAC as surrogate substrate. a) FT mass spectra of the free AdmF (yellow) using the octatrienoyl-*S*-NAC as substrate, leading to the formation of acylated-AdmF (blue). b) Octatrienoyl-*S*-NAC feeding of *E. coli* host cells expressing the *admA* gene knockout of the andrimid biosynthetic cluster. Liquid cultures of the cells mentioned above were grown in the presence of 200 μM octatrienoyl-*S*-NAC and incubated at 30 °C for 24 h. The resulting liquid medium was extracted with ethyl acetate and submitted to preparative HPLC (see Methods). Cells that were not fed the octatrienoyl-*S*-NAC did not produce any andrimid, as illustrated by the absence of a clearing zone of the bioassay plate and absence of a peak on the corresponding HPLC trace (see no. 1). Cells that were fed the octatrienoyl-*S*-NAC produced both antibiotic activity and a peak that coeluted with an authentic andrimid standard (see HPLC traces and bioassays 2 and 3, respectively). Notably, the octatrienoyl-*S*-NAC did not possess any apparent antibiotic activity (bioassay 4).